BBA - Biomembranes 1861 (2019) 256–267

Contents lists available at ScienceDirect

BBA - Biomembranes

journal homepage: www.elsevier.com/locate/bbamem

Antimicrobial and anti-inflammatory activities of chemokine CXCL14-derived antimicrobial peptide and its analogs

Ganesan Rajasekaran[a], S. Dinesh Kumar[a], Jiyoung Nam[b], Dasom Jeon[c], Yangmee Kim[c], Chul Won Lee[b], Il-Seon Park[a], Song Yub Shin[a,*]

[a] Department of Cellular and Molecular Medicine, Chosun University, Gwangju 61452, Republic of Korea
[b] Department of Chemistry, Chonnam National University, Gwangju 61186, Republic of Korea
[c] Department of Bioscience and Biotechnology, Konkuk University, Seoul 05029, Republic of Korea

ARTICLE INFO

Keywords:
CXCL14-C17
Antimicrobial activity
Anti-inflammatory activity
Cell selectivity
Antibiotic-resistant bacteria
Antimicrobial mechanism

ABSTRACT

CXCL14 is a CXC chemokine family that exhibits antimicrobial activity and contains an amphipathic cationic α-helical region in the C-terminus, a characteristic structure of antimicrobial peptides (AMPs). In this study, we designed three analogs of $CXCL14_{59–75}$ (named CXCL14-C17) corresponding to the C-terminal α-helix of CXCL14, which displayed potential antimicrobial activity against a wide variety of gram-negative and gram-positive bacteria with minimum inhibitory concentrations of 4 − 16 μM without mammalian cell toxicity. Furthermore, two CXCL14-C17 analogs (CXCL14-C17-a1 and CXCL14-C17-a3) with improved cell selectivity were engineered by introducing Lys, Arg, or Trp in CXCL14-C17. Additionally, CXCL14-C17 analogs showed much greater synergistic effect (FICI: 0.3125–0.375) with chloramphenicol and ciprofloxacin against multidrug-resistant *Pseudomonas aeruginosa* (MDRPA) than LL-37 did (FICI: 0.75–1.125). CXCL14-C17 analogs were more active against antibiotic-resistant bacteria including methicillin-resistant *Staphylococcus aureus* (MRSA), MDRPA, and vancomycin-resistant *Enterococcus faecium* (VREF) than LL-37 and melittin. In particular, CXCL14-C17-a2 and CXCL14-C17-a3 completely inhibited the biofilm formation at sub-MIC and all of the peptides were able to eliminate pre-formed biofilm as well. Membrane depolarization, flow cytometry, sytox green uptake, ONPG hydrolysis and confocal microscopy revealed the possible target of the native peptide (CXCL14-C17) to likely be intracellular, and the amphipathic designed analogs targeted the bacterial membrane. CXCL14-C17 also showed DNA binding characteristic activity similar to buforin-2. Interestingly, CXCL14-C17-a2 and CXCL14-C17-a3 effectively inhibited the production and expression of nitric oxide (NO), tumor necrosis factor (TNF)-α, interleukin (IL)-6, and monocyte chemoattractant protein (MCP)-1 from lipopolysaccharide (LPS)-stimulated RAW264.7 cells, suggesting that these peptides could be promising anti-inflammatory and antimicrobial agents.

1. Introduction

Chemokines belong to a superfamily of small globular proteins (8–14 kDa) that are pro-inflammatory mediators and potent leukocyte chemoattractants in human and mouse cells. They have four cysteines residues, which are conserved among all identified chemokines. Depending on the arrangement of these cysteine residues, two major chemokine groups have been categorized as the CC family with the first two cysteines adjacent to each other, and the CXC chemokine family that has one amino acid residue between the two cysteines [1]. One of the most recent characterized chemokine is CXCL14, which consists of 77 amino acid residues including four cysteines. Interestingly, CXCL14 possesses structural similarities with both the defensin family (anti-parallel β-sheets) and the cathelicidins (C-terminally located α-helix). In particular, the C-terminal α-helical region of CXCL14 shows a striking structural similarity with the human cathelicidin AMP LL-37 [2]. Because of its high positive charge at neutral pH, CXCL14 has a potent and broad-spectrum antimicrobial activity against gram-positive and gram-negative bacteria and *Candida albicans* [3]. It was reported that the C-terminal α-helical region of CXCL14 mediates its microbicidal activity [4].

In this study, we synthesized a 17-meric $CXCL14_{59–75}$ (CXCL14-C17) corresponding to the C-terminal α-helical region of CXCL14. CXCL14-C17 was found to exhibit potent antimicrobial activity (MIC range: 4 − 16 μM) without hemolytic activity even at high peptide concentration of 1024 μM (i.e., high cell selectivity). Although natural AMPs are exceptional in overcoming multidrug resistance, issues such as enzymatic degradation, production cost and cytotoxicity are serious

* Corresponding author.
E-mail address: syshin@chosun.ac.kr (S.Y. Shin).

https://doi.org/10.1016/j.bbamem.2018.06.016
Received 2 May 2018; Received in revised form 21 June 2018; Accepted 25 June 2018
Available online 28 June 2018

obstructions to further development of natural peptides as therapeutic drugs. Various approaches have been employed to optimize the native sequence of AMPs to improve antimicrobial effects while reducing cytotoxic effects in mammalian cells. The rational design of novel peptides with optimized structural properties and the chemical manipulation of existing ones represent valid approach to overcome the limitations of native peptides. In order to develop novel CXCL14-C17 analogs with a dual function of antimicrobial and anti-inflammatory activities, three CXCL14-C17 analogs were designed and synthesized by introducing Lys, Arg, or Trp (CXCL14-C17-a1, a2, and a3) based on the α-helical wheel diagram of CXCL14-C17. We evaluated the antimicrobial activity of CXCL14-C17 and its analogs against methicillin-resistant *Staphylococcus aureus* (MRSA), multidrug-resistant *Pseudomonas aeruginosa* (MDRPA) and vancomycin-resistant *Enterococcus faecium* (VREF). The ability of CXCL14-C17 and its analogs to inhibit the formation of bacterial biofilm against MDRPA was investigated. In addition, the synergistic effects of these peptides with conventional antibiotics against MDRPA were investigated. Furthermore, in order to understand the antimicrobial mechanism of CXCL14-C17 and its analogs, membrane depolarization, confocal laser scanning microscopy, flow cytometry and gel retardation were measured. Finally, the anti-inflammatory activity of CXCL14-C17 and its analogs was established by measuring their ability to suppress the release of nitric oxide (NO), tumor necrosis factor (TNF)-α, interleukin-6 (IL-6), and monocyte chemo-attractant protein-1 (MCP-1) from LPS-stimulated mouse macrophage RAW264.7 cells, as well as to reduce the mRNA levels of TNF-α, inducible nitric oxide synthase (iNOS), IL-6, and MCP-1 in these cells.

2. Materials and methods

2.1. Materials

Rink amide-methylbenzhydrylamine (MBHA) resin and 9-fluorenyl-methoxycarbonyl (Fmoc) protected amino acids used for solid phase peptide synthesis (SPPS) were purchased from Novabiochem (La Jolla, CA, USA). LPS purified from *Escherichia coli* O111:B4, 3-(4,5-dimethylthiazol-2-yl)-2,5-diphenyl-2H-tetrazolium bromide (MTT), ciprofloxacin, oxacillin and chloramphenicol, 3,3′-dipropyl-thiadicarbocyanine iodide ($diSC_3$–5) were supplied from Sigma-Aldrich (St. Louis, MO, USA). The TNF-α, IL-6 and MCP-1 kit was procured from R&D Systems (Minneapolis, MN, USA).

2.2. Peptide synthesis

The peptides were synthesized by Fmoc/tBu SPPS. The purity of the peptides (> 95%) was assessed by RP-HPLC on an analytical Vydac C_{18} column. Matrix-assisted laser desorption ionization-time-of-flight (MALDI-TOF) mass spectrometry (Shimadzu, Kyoto, Japan) was used to confirm the molecular mass of the synthesized peptides.

2.3. Bacterial strains

Three strains of gram-positive bacteria (*Bacillus subtilis* [KCTC 3068], *Staphylococcus epidermidis* [KCTC 1917], and *Staphylococcus aureus* [KCTC 1621]) and three strains of gram-negative bacteria (*Escherichia coli* [KCTC 1682], *Pseudomonas aeruginosa* [KCTC 1637], and *Salmonella typhimurium* [KCTC 1926]) were procured from the Korean Collection for Type Cultures (KCTC) of the Korea Research Institute of Bioscience and Biotechnology (KRIBB). Methicillin-resistant *Staphylococcus aureus* strains (MRSA; CCARM 3089, CCARM 3090, and CCARM 3095) and multidrug-resistant *Pseudomonas aeruginosa* strains (MDRPA; CCARM 2095, and CCARM 2109) were obtained from the Culture Collection of Antibiotic-Resistant Microbes (CCARM) of Seoul Women's University in Korea. Vancomycin-resistant *Enterococcus faecium* (VREF; ATCC 51559) was supplied from the American Type Culture Collection (Manassas, VA, USA).

2.4. Antimicrobial activity

Minimal inhibitory concentrations (MICs) of the peptides against standard bacteria and drug-resistant bacteria were determined by the standard broth micro dilution method as previously described [5]. MIC values were expressed in micromolar and correspond to the lowest concentration that inhibited the growth of the microorganism. In order to assess the effects of different salts and human serum on the antimicrobial activity of the peptides, MICs were also determined in the presence of salts and human serum. *E. coli* (KCTC 1682) or *S. aureus* (KCTC 1621) at a concentration of 2×10^6 CFU/ml were treated with peptides in 1% peptone containing physiological concentrations of various salts (150 mM NaCl or 4.5 mM KCl or 6 μM NH_4Cl or 1 mM $MgCl_2$ or 2.5 mM $CaCl_2$) or 20% human serum.

2.5. Hemolytic activity

Fresh human red blood cells (hRBCs) were washed three times with PBS (35 mM phosphate buffer, 0.15 M NaCl, pH 7.4) and centrifuged for 5 min at 116 ×*g*. A two-fold serial dilution of the peptides in PBS (the concentration test range was 2–512 μM) was added to each well of a 96-well plate. An equal volume of a 4% *w/v* hRBC suspension in PBS was added to each well. The plate was incubated for 1 h at 37 °C, and then the cells were pelleted by centrifugation at 1000 ×*g* for 5 min. The supernatants were transferred to clear 96-well plates. Hemoglobin was detected by measuring absorbance at 414 nm.

2.6. Circular dichroism (CD) spectroscopy

CD spectroscopy was carried out with a J-715 CD spectrophotometer (JASCO, Tokyo, Japan) using a 1 mm path length. The diluted peptide solution was sonicated (10 s) and vortexed prior to each use. CD Spectra were monitored with 1-mm-path length quartz cell at 1-nm data intervals. 1-s integration time and 3-scan accumulation. Spectra were acquired between 190 and 250 nm wavelengths at 25 °C. Peptides were analyzed at 100 μg/ml concentration in 10 mM sodium phosphate (pH 7.2) and 0.1% (0.22 mM) of *E. coli* LPS. Mean residue ellipticities were expressed as [θ] (deg·cm^2/dmol). The spectra of three consecutive scans were averaged, and the CD spectra of PBS buffer or LPS solutions without the peptide were used as baseline spectra. The CD spectra of the appropriate solvent were subtracted from each corresponding peptide spectrum. The percentage of helicity was calculated using the equation, % α-helix = -100 $(\theta_{222} + 3000)/33{,}000$, proposed by McLean et al. [6].

2.7. Synergy with conventional antibiotics

Antimicrobial interactions between the peptides and conventional antibiotics were evaluated via the chequerboard assay as described elsewhere [7]. Briefly, 2-fold serial dilutions of each antibiotic and each peptide were prepared and added in a 1:1 ratio. An equal volume of bacterial solution at ~10^6 CFU/ml was then seeded into each well. The plates were incubated in a shaking incubator at 37 °C and 200 rpm and read after 72 h. Bacterial growth was assessed visually or spectrophotometrically via OD_{600} readings.

2.8. Biofilm inhibition assay

Biofilm quantification was carried out as described elsewhere [5]. Briefly, 1×10^6 CFU/200 μl of MDRPA strain (CCARM 2095) in Mueller–Hinton broth (MHB) with 0.2% glucose were incubated at 37 °C for 24 h, in 96-well microtiter plates, with or without peptides. After the incubation, the planktonic bacteria were removed by washing three times with PBS solution. Afterwards, 99% methanol was added and

fixed for 15 min. After aspiration, the plates were allowed to dry. Dried wells were stained with 100 µl of 0.1% crystal violet for 5 min and excess stain was gently rinsed off with tap water. Stain was re-solubilized in 95% ethanol and absorbance at 600 nm was measured.

2.9. Biofilm eradication assay

Biofilms of MDRPA strain (CCARM 2095) were grown in 96-well plate by adding 100 µl of bacteria (1×10^5) in MHB media supplemented with 0.2% Glucose. Plates were incubated at 37 °C, 100 rpm for 24 h. The wells containing biofilm were washed three times with PBS. Peptides were serially diluted on a fresh 96-well plate using same media and 100 µl was transferred to the biofilm containing plate. 100 µl sterile media was added to the negative control wells. Plates were then incubated in a shaking incubator for 24 h at 37 °C, 100 rpm. After incubation, the wells were emptied and washed three times with µl of 200 PBS and air fixed for 1 h under aseptic condition. The percentage of biofilm removal was quantified by measuring the absorbance after applying crystal violet stain as described previously.

2.10. Membrane depolarization

Staphylococcus aureus (KCTC 1621) grown at 37 °C with agitation to the mid-log phase (OD_{600} = 0.4) was harvested by centrifugation. Cells were washed twice with washing buffer (20 mM glucose and 5 mM HEPES, pH 7.4) and resuspended to an OD_{600} of 0.05 in the same buffer. The cell suspension was incubated with 20 nM $diSC_3$–5 until a stable fluorescence value was achieved, implying the full incorporation of the dye into the bacterial membrane. Membrane depolarization was monitored based on the changes in the intensity of the fluorescence emitted from the $diSC_3$–5 (excitation λ = 622 nm, emission λ = 670 nm) after peptide addition. The membrane potential was fully abolished by adding gramicidin D at a final concentration of 0.2 nM.

2.11. ONPG hydrolysis assay

Inner membrane permeabilization was investigated by ONPG hydrolysis [8,9]. *Escherichia coli* ML-35 were grown to exponential phase in LB medium, washed with an equal volume of buffer (10 mM sodium phosphate (pH 7.4) containing 100 mM NaCl) and diluted in same buffer supplemented with 1.5 mM ONPG and peptides with different concentrations. The hydrolysis of ONPG to o-nitrophenol over time was monitored spectrophotometrically at 405 nm.

2.12. SYTOX green uptake assay

The effect of the peptides on bacterial membrane permeabilization was evaluated using the SYTOX green uptake assay as previously described [5,10]. *E. coli* (KCTC 1621) in exponential phase (A_{600} = 0.5) was collected and washed 3 times with a buffer containing 5 mM HEPES (pH 7.4) and 20 mM glucose. Cell suspensions were diluted to 1×10^6 CFU/ml in 5 mM HEPES (pH 7.4), 20 mM glucose, and 100 mM KCl. Bacterial suspensions were incubated with 0.5 µM SYTOX Green for 15 min in the dark. Then peptides were added to a final concentration equal to 2 × MIC and the uptake of SYTOX Green was monitored using a Shimadzu RF-5300PC fluorescence spectrophotometer (Shimadzu Scientific Instruments, Kyoto, Japan), with filter wavelengths of 485 and 520 nm for excitation and emission, respectively. This is possible because the cationic dye, which can only cross compromised membranes, binds to intracellular DNA and this interaction results in a significant increase of fluorescence intensity. Bacteria treated with melittin (a toxin from bee venom) and LL-37 were used as positive controls to provide maximal permeabilization values.

2.13. Flow cytometry

Mid logarithmic phase of *Escherichia coli* (KCTC 1682) cells were harvested and washed three times with PBS buffer and resuspended in the same buffer to OD = 0.3. Bacteria were incubated with (2 × MIC) or without peptide for 1 h at 37 °C. Cells were centrifuged and incubated with PI (propidium iodide, 10 µg/ml) for 30 min at 4 °C. Afterwards, bacteria cells were centrifuged at 10,000 × *g* and re-suspended in 1 ml of PBS. Analysis was performed using a Cyto FLEX flow cytometer (Beckman Coulter, Brea, CA USA).

2.14. Confocal laser-scanning microscopy

Escherichia coli (KCTC 1682) cells in the mid-logarithmic phase were harvested by centrifugation, washed three times with a 10-mM phosphate buffer saline, pH 7.4. Bacteria (10^7 CFU/ml) cells were incubated with FITC-labeled peptides (2 × MIC) at 37 °C for 30 min. After being incubated, the bacterial cells were pelleted down and washed three times with the 10 mM sodium phosphate buffer, pH 7.4, and immobilized on a glass slide. The FITC-labeled peptides were observed with a Zeiss Axioplan 2 optical microscope (Japan). Fluorescent images were obtained with a 488-nm band-pass filter for excitation of FITC.

2.15. Gel retardation assay

Gel retardation assay was used to identify that peptides ability to interact with DNA by binding to them. Briefly, increasing amounts of peptides were mixed with 200 ng of plasmid DNA (pBR322) in buffer containing 10 mM Tris-HCl, 5% glucose, 50 µg/ml BSA, 1 mM EDTA and 20 mM KCl. Wells containing only plasmid served as negative control. The peptide and plasmid mixture was incubated at 37 °C water bath for 30 mins and then separated by agarose gel electrophoresis (1% agarose) in 0.5% TAE buffer. Afterwards, DNA bands were visualized by UV illumination using Bio-Rad Gel documentation system.

2.16. Cytotoxicity assay against RAW264.7 cells

RAW264.7 cells were cultured in Dulbecco's modified Eagle's medium supplemented with 10% fetal calf serum at 37 °C under a 5% CO_2 atmosphere. Growth inhibition was evaluated using MTT assay to measure cell viability. The cells were seeded in 96-well plates (2×10^4 cells/well) and cultured for 24 h at 37 °C. Increasing concentrations of the peptides were added and allowed to react with the cells for 48 h, followed by the addition of 20 µl MTT (5 mg/ml in PBS) for another 4 h at 37 °C. Formazan crystals were dissolved in DMSO and absorbance at 550 nm was measured.

2.17. Production of nitric oxide (NO) from LPS-stimulated RAW264.7 cells

RAW264.7 cells were plated at a density of 5×10^5 cells/ml in 96-well culture plates and stimulated with LPS (20 ng/ml) in the presence or absence of peptides for 24 h. Isolated supernatant fractions were mixed with an equal volume of Griess reagent (1% sulfanilamide, 0.1% naphthylethylenediamine dihydrochloride and 2% phosphoric acid) and incubated at room temperature for 10 min. Nitrite production was quantified by measuring absorbance at 540 nm, and concentrations were determined using a standard curve generated with $NaNO_2$.

2.18. Release of cytokines from LPS-stimulated RAW264.7 cells

RAW264.7 cells were seeded in 96-well plates (5×10^4 cells/well) and incubated overnight. Peptides were added and the cultures were incubated at 37 °C for 1 h. Subsequently, 20 ng/ml LPS was added and the cells were incubated for another 6 h at 37 °C. Levels of TNF-α, IL-6 and MCP-1 in the samples were measured by the commercial enzyme-linked immunosorbent assay kit (R&D Systems, Minneapolis, MN, USA)

according to the manufacturer's instructions.

2.19. Reverse-transcription polymerase chain reaction (RT-PCR)

RAW264.7 cells were plated at a concentration of 5×10^5 cells/well in six-well plates and incubated overnight. Various concentrations of peptide and/or LPS (20 ng/ml) was added to the wells. The primers used were purchased from Bioneer (Seoul, Korea). The cDNA products were amplified in the presence of primers for iNOS (forward, 5′-CTGC AGCACTTGGATCAGGAACCTG-3′; reverse, 5′-GGAGTAGCCTGTGTGC ACCTGGAA-3′), TNF-α (forward, 5′-CTGCAGCACTTGGATCAGGAAC CTG-3′; reverse, 5′-GGGAGTAGCCTGTG TGCACCTGGAA-3′), IL-6 (forward, 5′-ACAACCACGGCCTTCCCTACTT-3′; reverse, 5′-CACGATTT CCCAGAGAACATGTG-3′), MCP-1 (forward, 5′-ATCCCAATGAGTAGGC TGGAGAGC-3′; reverse, 5′-CAGAAGTGCTTGAGGTGGTTGTG-3′), and GAPDH (forward, 5′-GACATCAAGAAGGTGGTGAA-3′; reverse, 5′-TGT CATACCAGGAAATG AGC-3′). The amplification protocol consisted of an initial denaturation step of 5 min at 94 °C, followed by 30 cycles of denaturation at 94 °C for 1 min, annealing at 55 °C for 1.5 min, and extension at 72 °C for 1 min, and afterwards by a final extension step of 5 min at 72 °C.

2.20. Statistical analysis

All results are presented as averages of values derived from three independent experiments, with triplicates used in each experiment. Error bars represent the mean ± standard deviation of the mean. The statistical significance of differences between samples and respective controls (no added antimicrobial agent) were determined by one-way analysis of variance (ANOVA) with Bonferroni's post-test method using Sigma plot v12.0 (Systat Software Inc., San Jose, CA, USA). Differences with $p < 0.001$ were considered statistically significant.

3. Results and discussion

3.1. Peptide design

The amino acid sequences of CXCL14-C17 and its analogs generated in this study are summarized in Table 1. The design of the peptide analogs was based on the α-helical-wheel diagram and three-dimensional structure of CXCL14-C17 (Fig. 1). CXCL14-C17 could not adopt the amphipathic α-helical structure since the hydrophobic and positively charged residues are dispersed all around the molecule (Fig. 1b). The cationic side chains such as Arg or Lys in antimicrobial peptides (AMPs) facilitate their interaction with negatively charged bacterial membranes. Trp may ensure a stronger interaction with membrane surfaces, allowing the peptides to be partitioned into the lipid bilayer interface rather than other hydrophobic residues such as Leu, Ile, Phe, and Tyr [11,12]. The α-helical AMPs with idealized facial amphipathicity comprising continuous hydrophobic and hydrophilic faces without interrupted segments, provide optimal cell selectivity [13,14]. Therefore, CXCL14-C17-a1 was designed by replacing Asn^8 and Glu^{12} in CXCL14-C17 with Lys to increase the net positive charge of the peptide and to form a continuous positive face on the left side of the molecule (Fig. 1b). Moreover, CXCL14-C17-a2 was designed by substituting Arg^{14} and Val^{16} in CXCL14-C17-a1 with Trp and Lys, respectively, to increase the amphipathicity of the peptide having a continuous hydrophobic face on the right side of the molecule (Fig. 1b). Finally, $Ile^4 \longrightarrow$ Lys and $Asn^{11} \longrightarrow$ Arg substitution in CXCL14-C17-a2 produced CXCL14-C17-a3, which achieved the desired idealized facial amphipathicity of the peptide. The synthetic peptides were amidated at the C-terminus to improve the antimicrobial activity by increasing the net positive charge [15].

3.2. Antimicrobial activity

The antimicrobial activity of the peptides against both gram-negative and gram-positive bacteria was evaluated by determining the minimum inhibitory concentrations (MICs) (Table 2). The antimicrobial activity of the peptide was evaluated overall by determining the geometric mean (GM) of the MICs against six bacterial strains (Table 3). The GM values of all analogs displayed a 2–4-fold increased antimicrobial activity compared to that of CXCL14-C17. The antimicrobial potency was ranked according to the GM as follows: CXCL14-C17-a3 > CXCL14-C17-a1 = CXCL14-C17-a2 > CXCL14-C17.

3.3. Hemolytic activity

The cytotoxicity of the peptides was evaluated by analyzing the hemolytic activity against human red blood cells (hRBCs). For the measurement of the hemolytic activity of the peptides, we determined the minimal hemolytic concentration (MHC) defined as the lowest peptide concentration that produces 10% hemolysis against hRBCs (Fig. 2 and Table 3). All peptides showed no or < 5% hemolytic activity at the high concentration of 256 μM. As shown in Fig. 2, CXCL14-C17 and CXCL14-C17-a1 did not induce 10% hemolysis even at the highest concentration tested (1024 μM). CXCL14-C17-a2 and CXCL14-C17-a3 showed 10% hemolysis at 480 μM and 700 μM, respectively.

3.4. Cell selectivity

The therapeutic index (TI) was calculated as the ratio of MHC value of the peptides to their GMs (Table 3). TI is a parameter that is used to describe the cell selectivity of antimicrobial agents between bacterial and mammalian cells [16,17]. A larger TI value indicates greater cell selectivity. The TI values of the peptides are shown in Table 3. Of the four synthesized peptides, CXCL14-C17-a1 and CXCL14-C17-a3 showed superior cell selectivity, with TI values of 553.5 and 350.0, which were 1.37- and 2.16-fold higher than that of CXCL14-C17 (TI = 256.0), respectively.

3.5. Antimicrobial activity against antibiotic-resistant bacteria

Recently, severe infections caused by multidrug-resistant bacteria have become a major challenge for conventional antibiotic treatments. Therefore, we examined the antimicrobial activity of the peptides

Table 1
Amino acid sequences and physicochemical properties of 17-meric $CXCL14_{59–75}$ (CXCL14-C17) and its analogs.

Peptides	Amino acid sequence	Molecular weight (Da)		Net charge
		Calculated	Observed[a]	
CXCL14-C17	KRFIKWYNAWNEKRRVY-NH_2	2356.8	2356.6	+5
CXCL14-C17-a1	KRFIKWY**K**AWN**K**KRRVY-NH_2	2369.9	2369.4	+8
CXCL14-C17-a2	KRFIKWY**K**AWN**K**K**W**R**K**Y-NH_2	2428.9	2428.3	+8
CXCL14-C17-a3	KRF**K**KWY**K**AW**R**K**W**R**K**Y-NH_2	2486.0	2485.4	+10

The substituted amino acids are shown bold and underlined.
[a] Molecular mass were determined using matrix-assisted laser desorption/ionization (MALDI)-time-of-flight (TOF)-mass spectrometry (MS).

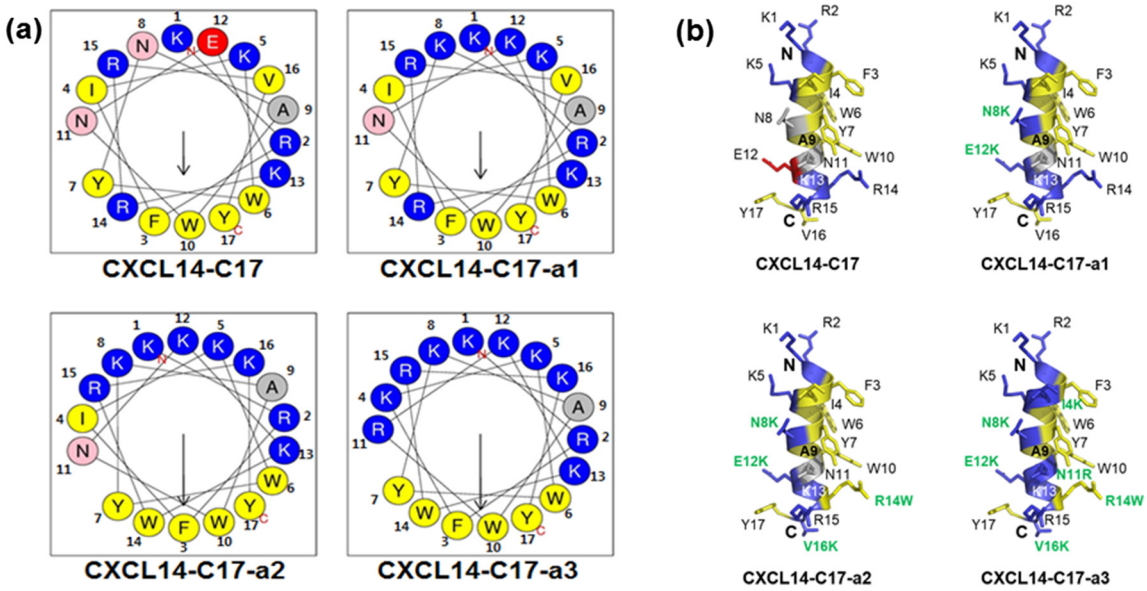

Fig. 1. (a) Helical wheel projection diagrams of 17-meric $CXCL14_{59–75}$ (CXCL14-C17) and its analogs. Positively charged residues (polar) are represented as blue circles and hydrophobic (nonpolar) residues are yellow circles. (b) The helix structure of CXCL14-C17 derived from the NMR structure of full-length CXCL14 (PDB ID: 2HDL). Positively charged and hydrophobic residues are represented as blue and yellow, respectively. The substitution positions of the analogs are indicated by green letters and residue characteristic color after substitution in the structure of CXCL14-C17. (For interpretation of the references to color in this figure legend, the reader is referred to the web version of this article.)

Table 2
Minimum inhibitory concentration (MIC) values for the peptides used in this study.

Peptides	MIC[a] (μM)					
	Escherichia coli [KCTC 1682]	*Pseudomonas aeruginosa* [KCTC 1637]	*Salmonella typhimurium* [KCTC 1926]	*Bacillus subtilis* [KCTC 3068]	*Staphylococcus epidermidis* [KCTC 1917]	*Staphylococcus aureus* [KCTC 1621]
CXCL14-C17	8	16	4	8	8	4
CXCL14-C17-a1	4	2	2	8	4	2
CXCL14-C17-a2	4	2	2	8	4	2
CXCL14-C17-a3	2	2	1	4	2	1

[a] MICs were determined as the lowest concentration of peptide that inhibited bacteria growth.

Table 3
Geometric mean (GM), minimum hemolytic concentration (MHC), and therapeutic index (TI) of the peptides used in this study.

Peptides	GM (μM)[a]	MHC (μM)[a]	TI (MHC/GM)[b]
CXCL14-C17	8.0	> 1024	256
CXCL14-C17-a1	3.7	> 1024	553.5
CXCL14-C17-a2	3.7	480	129.7
CXCL14-C17-a3	2.0	700	350.0

When 10% hemolysis was not observed at 1024 μM, a value of 2048 μM was used for calculation of MHC.

[a] The MHC is the minimum hemolytic concentration that caused 10% hemolysis of human red blood cells (hRBCs).

[b] Therapeutic index (TI) is the ratio of the MHC value (μM) to GM (μM).

against antibiotic-resistant bacteria, which were three methicillin-resistant *Staphylococcus aureus* (MRSA), two multidrug-resistant *Pseudomonas aeruginosa* (MDRPA), and a vancomycin-resistant *Enterococcus faecium* (VREF) strain (ATCC 51559) (Table 4). Remarkably, CXCL14-C17 and its analogs exhibited potent activity with MICs ranging from 2 to 16 μM against tested drug-resistant pathogens. All CXCL14-C17 analogs showed stronger (2- to 4-fold) antimicrobial activity against all tested antibiotic-resistant bacterial strains than the natural AMPs, LL-37, and melittin.

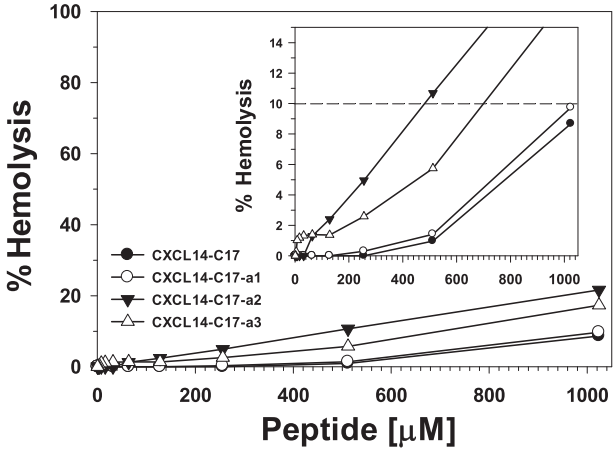

Fig. 2. Dose-response curves of hemolysis against human red blood cells (hRBCs) induced by 17-meric $CXCL14_{59–75}$ (CXCL14-C17) and its analogs. Value of "zero hemolysis" was determined using phosphate-buffered saline (PBS, A_{PBS}) while 100% hemolysis was established using 0.1% (*v*/*v*) Triton X-100 (A_{Triton}). Percentage hemolysis was calculated as follows: hemolysis % = $[(A_{Sample} - A_{PBS}) / (A_{Triton} - A_{PBS})] \times 100$.

Table 4
Antimicrobial activities of the peptides against antibiotic-resistant bacteria.

Microorganisms	MIC (μM)					
	CXCL14-C17	CXCL14-C17-a1	CXCL14-C17-a2	CXCL14-C17-a3	LL-37	melittin
MRSA[a]						
CCARM 3089	8	4	2	2	16	8
CCARM 3090	8	4	2	2	16	8
CCARM 3095	8	4	2	2	16	8
MDRPA[b]						
CCARM 2095	4	4	4	4	8	16
CCARM 2109	16	8	8	4	16	16
VREF[c]						
ATCC 51559	8	4	4	2	16	8

[a] MRSA: methicillin-resistant *Staphylococcus aureus*.
[b] MDRPA: multidrug-resistant *Pseudomonas aeruginosa*.
[c] VREF: vancomycin-resistant *Enterococcus faecium*.

3.6. The interaction of peptides and LPS

To study the propensity of the peptides to binding to LPS, the CD spectra were analyzed in free solution and in complex with LPS micelles. As shown in Fig. 3, all peptides showed an unordered conformation in PBS solution but exhibited conformational changes in LPS micelles, with two negative bands at 208 to 210 nm and at 220 to 225 nm, indicating predominantly α-helical conformations (Fig. 3-b). Flexibility and dynamics of peptides can adjust their conformation to the bacterial membrane environments [18]. Structural investigations show that the random coil structure of these peptides in aqueous solution becomes helical once the peptide inserts/binds into bacterial membrane environments. The calculated α-helical contents for CXCL14-C17, CXCL14-C17-a1, CXCL14-C17-a2, and CXCL14-C17-a3 were 3.0%, 7.1%, 20.9%, and 26.9% in LPS micelles, respectively (Table 5). These results suggest that the increase of α-helicity of the peptide on LPS is related to the increase of antimicrobial activity in gram-negative bacteria.

Table 5
Mean residual ellipticity at 222 nm ($[\theta]_{222}$) and percent α-helical contents of CXCL14-C17and its analogs in aqueous buffer and 0.1% LPS.

Peptide	Buffer		0.1% LPS	
	$[\theta]_{222}$	% α-helix	$[\theta]_{222}$	% α-helix
CXCL14-C17	−890.7	rc	−3976.3	3.0
CXCL14-C17-a1	−307.6	rc	−5344.6	7.1
CXCL14-C17-a2	−168.2	rc	−9911.3	20.9
CXCL14-C17-a3	−894.2	rc	−11,878.4	26.9

% α-helix = -100 ($[\theta]_{222}$ + 3000)/33,000. rc means random coli.

3.7. Salt and serum stability

In order to investigate the stability of the peptides were tested for antimicrobial activity against *E. coli* and *S. aureus* in the different environment including salt and human serum. Bacteria was treated with peptides supplemented with different salts at physiological concentrations (150 mM NaCl, 4.5 mM KCl, 6 μM NH_4Cl, 1 mM $MgCl_2$, and 2.5 mM $CaCl_2$) and as well as 20% human serum. Presence of salts could affect the MIC values of peptides, especially Mg^{2+} and Na^+. This impact was similar to both tested bacterial strains (*E. coli* and *S. aureus*). The decreased MICs might be caused by weak electrostatic interaction between peptides and membranes in the salt environment. As shown in Table 6, the effect was diverse depending on the peptide and the salt, with some peptide/salt combinations displaying activity similar to that of the peptide in the absence of salt, and others presenting a 2- to 8-fold decrease in activity. Generally, all CXCL14-C17 analogs tended to be more stable in the presence of physiological salts than CXCL14-C17. We also treated the bacteria with the peptides in the presence of 20% human serum. Human serum, as a mixture of all kinds of salts, had a dramatic reduced antimicrobial activity. As expected, two control AMPs (melittin and LL-37) and CXCL14-C17 and its analogs displayed a 4- to 16-fold decreased antimicrobial activity when supplemented with 20% human serum. Of the three CXCL14-C17 analogs, CXCL14-C17-a2 was

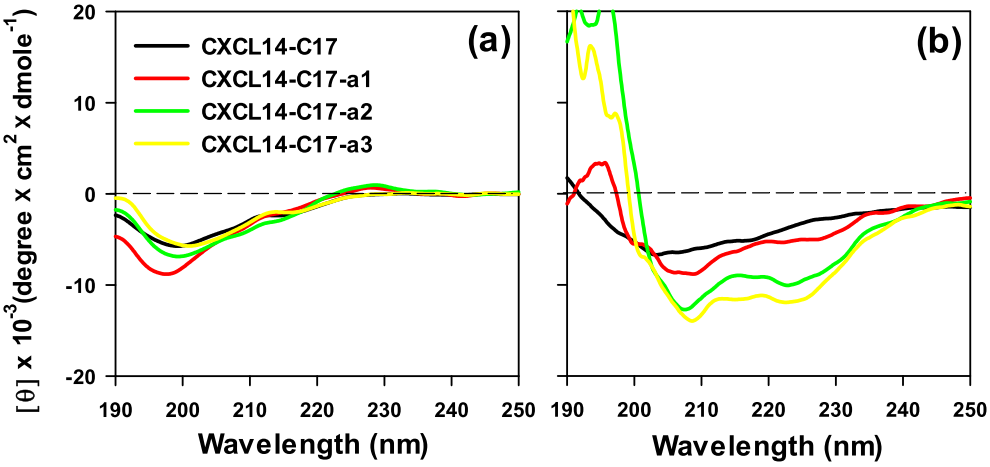

Fig. 3. The CD spectra of CXCL14-C17 and its analogs. The peptides were dissolved in 10 mM sodium phosphate buffer (a), 0.1% (0.22 mM) LPS (b). The mean residue ellipticity was plotted against wavelength. The values from three scans were averaged per sample.

Table 6
MIC values of the peptides in the presence of physiological salts and human serum (HS) against *E. coli* and *S. aureus*.

Peptides	Control	150 mM NaCl	4.5 mM KCl	6 μM NH_4Cl	1mM $MgCl_2$	2.5mM $CaCl_2$	20% HS
MIC (μM) against *E. coli* (KCTC 1682)							
CXCL14-C17	8	32	8	8	32	32	32
CXCL14-C17-a1	4	16	4	4	8	16	32
CXCL14-C17-a2	4	4	4	4	8	8	8
CXCL14-C17-a3	2	4	2	2	4	4	8
melittin	2	2	2	2	4	8	16
LL-37	8	8	8	4	16	16	32
MIC (μM) against *S. aureus* (KCTC1621)							
CXCL14-C17	4	32	4	4	8	32	32
CXCL14-C17-a1	2	2	2	2	4	4	32
CXCL14-C17-a2	2	2	2	2	4	4	8
CXCL14-C17-a3	1	2	2	2	4	4	8
melittin	1	1	1	1	1	1	16
LL-37	8	16	8	8	8	8	32

Control represents bacteria treated with peptide only.

more tolerant of human serum than the other analogs.

3.8. Synergism between peptides and conventional antibiotics

Combination antibiotic therapy has also been practiced for the effective treatment of routine bacterial infections [19,20]. The combined use of new AMPs with existing antibiotics could enhance the efficacy of conventional antibiotics and reduce the amount of peptide needed for treatment. Therefore, we used three conventional antibiotics with a different mechanism of antimicrobial action, namely chloramphenicol (a protein synthesis inhibitor), ciprofloxacin (a DNA gyrase inhibitor), and oxacillin (a cell wall synthesis inhibitor). The fractional inhibitory concentration index (FICI) data of the combinations of antibiotics and the peptides are shown in Table 7. Overall, CXCL14-C17 analogs showed a remarkable synergy with chloramphenicol and ciprofloxacin against MDRPA, with FICI values from 0.3125 to 0.375. In addition, these peptides showed an additive effect with oxacillin, with an FICI value of 0.625. However, CXCL14-C17 showed an additive effect with chloramphenicol and ciprofloxacin with FICI values of 0.75 and 0.5 respectively, whereas it showed an indifferent effect with oxacillin (FICI, 1.5). In particular, CXCL14-C17 analogs showed much higher synergistic effects with chloramphenicol and ciprofloxacin on MDRPA than on LL-37. This could be an impressive advantage for these molecules in preventing or delaying the potential acquisition of resistance.

Table 7
Fractional inhibitory concentration index (FICI)[a] of the peptides in combination with conventional antibiotics against multidrug-resistant *Pseudomonas aeruginosa* (MDRPA) (CCARM 2095).

Peptide	Chloramphenicol	Ciprofloxacin	Oxacillin
CXCL14-C17	0.75 (256/512 + 1/4)	0.50 (128/512 + 1/4)	1.50 (1024/1024 + 2/4)
CXCL14-C17-a1	0.3125 (128/512 + 0.25/4)	0.375 (128/512 + 0.5/4)	0.625 (512/1024 + 0.5/4)
CXCL14-C17-a2	0.3125 (128/512 + 0.25/4)	0.375 (128/512 + 0.5/4)	0.625 (512/1024 + 0.5/4)
CXCL14-C17-a3	0.375 (128/512 + 0.5/4)	0.375 (128/512 + 0.5/4)	0.625 (512/1024 + 0.5/4)
LL-37	1.125 (512/512 + 1/8)	0.75 (256/512 + 1/8)	1.50 (1024/1024 + 4/8)

[a] FICI = (MIC of antibiotic in combination)/(MIC of antibiotic alone) + (MIC of peptide in combination)/(MIC of peptide alone). FICI < 0.5 is synergy, 0.5 < FICI < 1.0 is additive, 1.0 < FICI < 4.0 is indifferent, and FICI > 4.0 is antagonism.

3.9. Biofilm inhibition and eradication activity

The ability of bacteria to produce biofilm is considered a serious threat, which contributes to disease pathogenesis and antibiotic resistance [21]. *P. aeruginosa* is known as a major biofilm-forming pathogen [22]. Therefore, we investigated the biofilm inhibition activity of the peptides against MDRPA (CCARM 2095) at sub-MICs. As shown in Fig. 4-a, CXCL14-C17-a2 and CXCL14-C17-a3 inhibited 90% and 60% of biofilm formation respectively at 0.5 × MIC. On the other hand, the control peptide LL-37 was able to inhibit only 10 − 20%. Since the bacteria that generate biofilm usually exhibit a distinct phenotype from that of planktonic cells, it was impressive that both CXCL14-C17-a2 and CXCL14-C17-a3 showed potent activity against planktonic cells and presented biofilm inhibition activity at sub-MIC levels. Eradicating preformed biofilm becomes major problem for any therapeutic agents. Fig. 4-b shows the eradication of a 24 h mature biofilm when subjected to increasing concentrations of peptide. Concentration required for all peptides to eradicate 10–50% of biofilm was 1 μM. Interestingly as the peptide concentration increased, more biofilm was eliminated. At 2 μM concentration, 50 − 80% of biofilm was eliminated and when treated with 8–16 μM concentration of peptides, 80–90% of biofilm was eradicated. This indicated that biofilm eradication was concentration dependent manner. Promisingly, CXCL14-C17-a1 was most active to eliminate preformed biofilm than other peptides even at low tested concentrations (0.125 to 1 μM). Overall, all of our synthesized peptides were strong biofilm eradicators than the control peptide LL-37.

3.10. Antimicrobial mechanism of action

To explore the antimicrobial mechanism of action of the peptides, their effects on the bacterial membranes were investigated using membrane depolarization, flow cytometry and confocal laser-scanning microscopy. $DiSC_3$–5, a membrane potential-dependent probe, is released into the medium when the membrane potential is disrupted, which increases the fluorescence. The peptide-induced depolarization was monitored over a period of 600 s, as shown in Fig. 5. Except for CXCL14-C17, all analogs induced cytoplasmic membrane depolarization at 2 × MIC. As expected, melittin and LL-37 known as the membrane-targeting AMP completely depolarized the cytoplasmic membrane at 2 × MIC. Similarly, buforin-2 known as an intracellular-targeting AMP did not induce membrane depolarization.

PI is a non-membrane permeable dye, and when the peptide damages the membrane integrity, PI binds to double-stranded DNA by intercalating between base pairs. As showed in Fig. 6, bacteria treated with CXCL14-C17-a1, CXCL14-C17-a2, and CXCL14-C17-a3 exhibited an increase in fluorescence intensity (36.81%, 47.61%, and 38.56% respectively), and the effects were similar to those of melittin (59.08%).

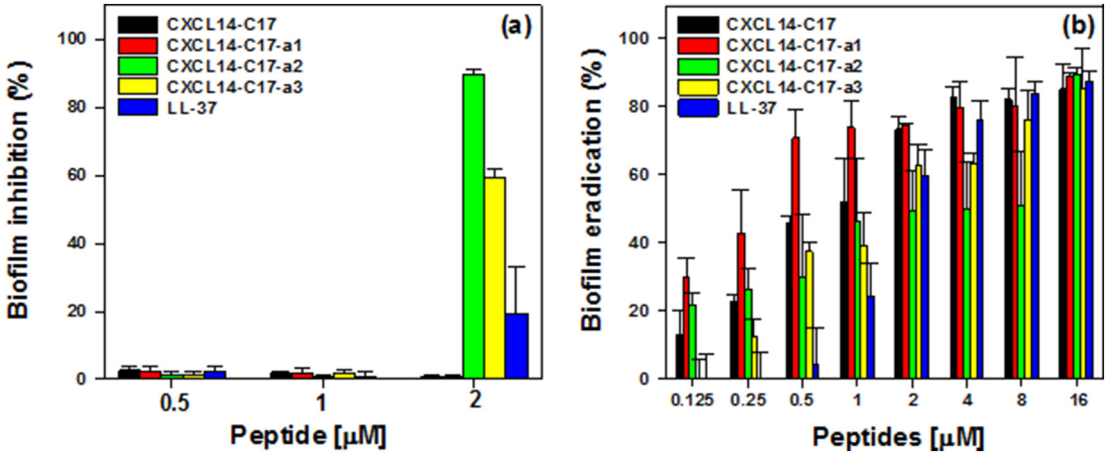

Fig. 4. (a) Inhibitory effect of 17-meric $CXCL14_{59–75}$ (CXCL14-C17) and its analogs on multidrug-resistant *Pseudomonas aeruginosa* (MDRPA) biofilm formation. MDRPA (CCARM 2095) was incubated for 24 h with indicated concentrations of peptides. After incubation, crystal violet was used to stain the biofilm. The stain was dissolved in 95% ethanol, and absorbance at 600 nm (OD_{600}) was measured. (b) *Pseudomonas aeruginosa* MDRPA biofilm eradication. Overnight bacterial cultures in MHB were diluted 1:100 in fresh MHB + glucose and plated in 96-well plates and biofilm was allowed to form overnight at 37 °C. Peptides were added to the preformed biofilm after removal of residual planktonic bacteria and allowed to react overnight. Then, crystal violet was used to stain the biofilm. The stain was dissolved in 95% ethanol, and absorbance at 600 nm (OD_{600}) was measured. Values are means ± SEM of technical triplicates. Data were analyzed using one-way analysis of variance (ANOVA) with Bonferroni's post-test. *Significant effect ($^*p < 0.001$ for each agonist) of the peptide compared to control (without peptide).

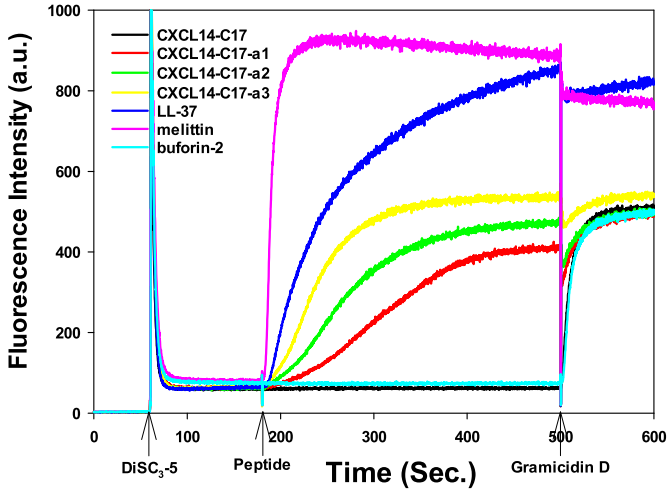

Fig. 5. Depolarization of *Staphylococcus aureus* cytoplasmic membrane induced by 17-meric $CXCL14_{59–75}$ (CXCL14-C17) and its analogs at 2 × MIC, determined using membrane potential-sensitive fluorescent dye $diSC_3$–5. Dye release was monitored by measuring fluorescence at an excitation and emission wavelengths of 622 and 670 nm, respectively and plotting the emission against time. Curves corresponding to positive control peptides (LL-37 and melittin) and negative control peptide (buforin-2) are also shown.

This observation suggests that the peptide analogs may have the potential to disrupt the bacteria membranes by pore formation. In contrast, the fluorescence intensity of CXCL14-C17 (5.69%) was similar to that of buforin-2 (6.41%), and the condition without the peptide (5.36%), indicating CXCL14-C17 was unable to damage the membrane integrity.

To investigate if synthesized peptides affect bacterial membrane integrity, *E. coli* permeability to the SYTOX green dye was studied. Cationic dye, SYTOX green can only cross compromised membranes, which later can bind with nucleic acids of bacterial cells and increases the fluorescence intensity. Thus, its accumulation inside bacterial cells indicates cytoplasmic membrane disruption. When 2 × MIC of peptides treated with bacteria, increased fluorescence intensity was observed, which indicated that direct emulating membrane permeabilization ability (Fig. 7). Like LL-37 and melittin, CXCL14-C17-a1, CXCL14-C17-a2 and CXCL14-C17-a3 analogs were able to permeate the membrane of *E. coli*, as indicated by the increase in fluorescence of samples treated with peptides compared to that of the negative controls (without peptide). However, as observed in buforin-2, CXCL14-C17 permeabilized poorly with a weak SYTOX Green fluorescence signal. This result indicated that CXCL14-C17 did not disrupt cytoplasmic membrane of *E. coli.* Overall, direct correlation was found between the potency of different peptide inducing the influx of SYTOX green into the cells and their corresponding antimicrobial activities on those cells.

Next, in order to execute membrane permeabilization, peptide translocation into inner membrane is one of the critical steps. We examined the ability of peptides to permeate inner (plasma) membrane using the lactose permease deficient strain *E. coli* ML-35. Inner membrane disruption was indicated by leakage of β-galactosidase to catalyze a nonchromogenic substrate ONPG to produce o-nitrophenol which can be detected at OD_{420}. As shown in Fig. 8, all CXCL14-C17 analogs induced a rapid increase in the permeability of inner membrane at their 2 × MICs, which is similar to the control peptides LL-37 and melittin. However, the parent peptide CXCL14-C17 induced a negligible inner membrane permeabilization, which is resembling to buforin-2. These results suggested that all CXCL14-C17 analogs damaged the inner cell membrane, but CXCL14-C17 was unable to do so.

Finally, the peptides were labeled with fluorescein isothiocyanate (FITC), and their localization in *E. coli* was examined using confocal *laser scanning* microscopy. The images shown in Fig. 9 reveal the translocation and localization of the peptides in the bacterial cytoplasm. Similar to buforin-2, the green fluorescence inside the bacterial cells was observed only following CXCL14-C17 treatment, suggesting that it penetrated the bacterial cell membrane, thereby killing them. Furthermore, green fluorescence was detected on the membrane of bacteria exposed to all analogs, suggesting that the peptides targeted the bacterial membrane.

After determining that CXCL14-C17 could translocate into the bacterial cell membrane, we attempted to identify the internal target of CXCL14-C17. One plausible mode of action is that the bacteria are killed by binding of the peptide to DNA. The binding affinity of buforin-2, which is well known to bind to plasmid DNA, was also evaluated and compared with that of the peptides. Various concentrations of the peptide were incubated with plasmid DNA, and at up to 2 μM, the plasmid migrated through the agarose gel similar to non-complexed DNA. In addition, following treatment with 4 μM and 8 μM buforin-2

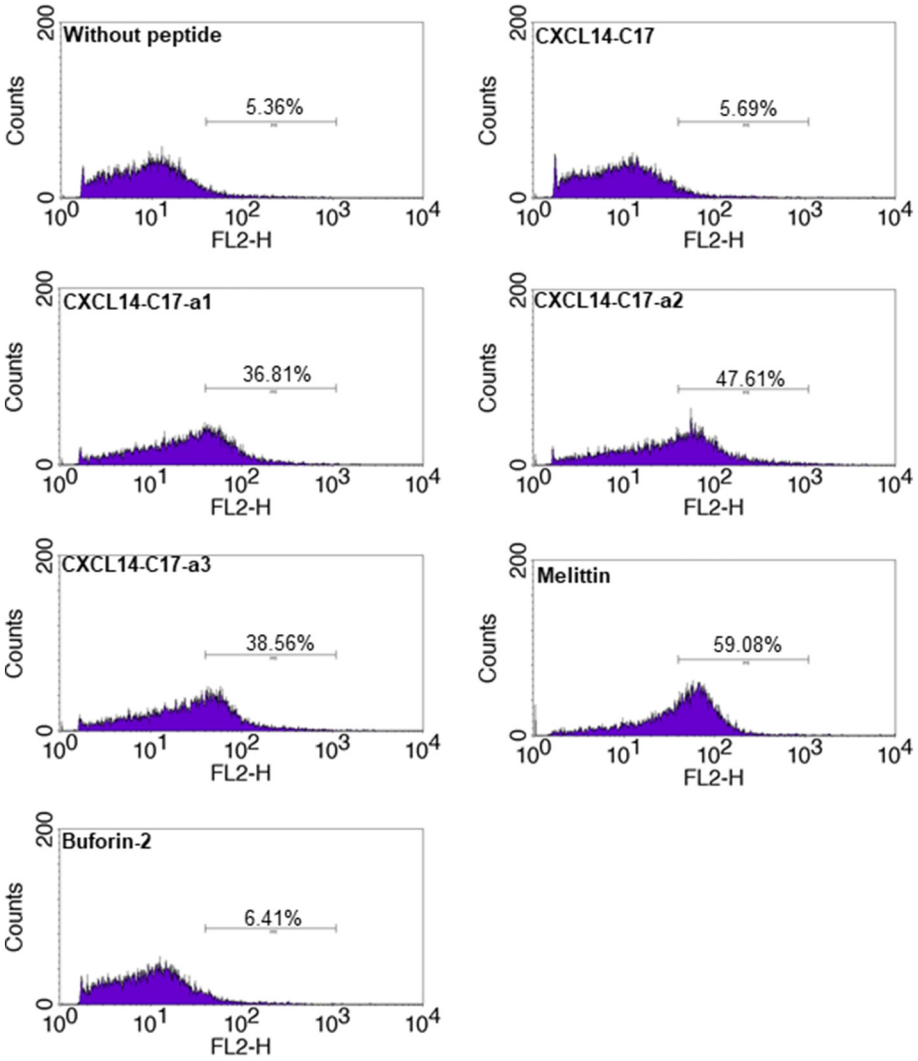

Fig. 6. The membrane damage of *Escherichia coli* cells treated by peptides (2 × MIC), as measured by an increase of fluorescent intensity of PI (10 μg/ml) at 4 °C for 30 min.

and CXCL14-C17 a fraction of the plasmid DNA was still able to migrate (Fig. 10). At higher concentration (16 μM) both peptides blocked the migration of plasmid DNA, suggesting that the peptides bind with DNA, thereby arresting and killing the bacterial cells.

3.11. Anti-inflammatory activity (endotoxin-neutralizing activity)

Lipopolysaccharide (LPS) is a major component of the outer membrane of gram-negative bacteria and elicits strong inflammatory

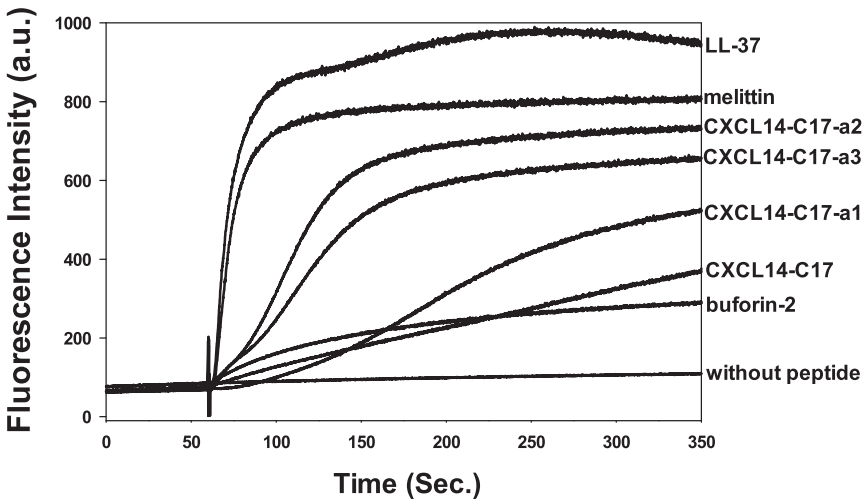

Fig. 7. Sytox green uptake. *E. coli* membrane permeabilization caused by CXCL14-C17 and its analogs at 2 × MIC. The positive control peptides (LL-37 and melittin) and negative control peptide (buforin-2 and without peptide) are also shown. Alterations of the cytoplasmic membrane allow the SYTOX Green probe to enter the cell and bind DNA, resulting in an increase of fluorescence. (For interpretation of the references to color in this figure legend, the reader is referred to the web version of this article.)

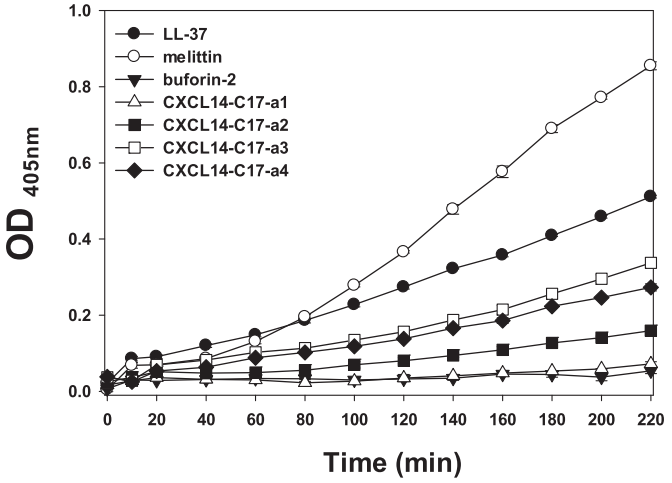

Fig. 8. The inner membrane permeability of the peptides. The hydrolysis of ONPG due to release of cytoplasmic β-galactosidase of *E. coli* ML-35 treated by 2 × MIC peptides was measured spectroscopically at absorbance of 420 nm as a function of time.

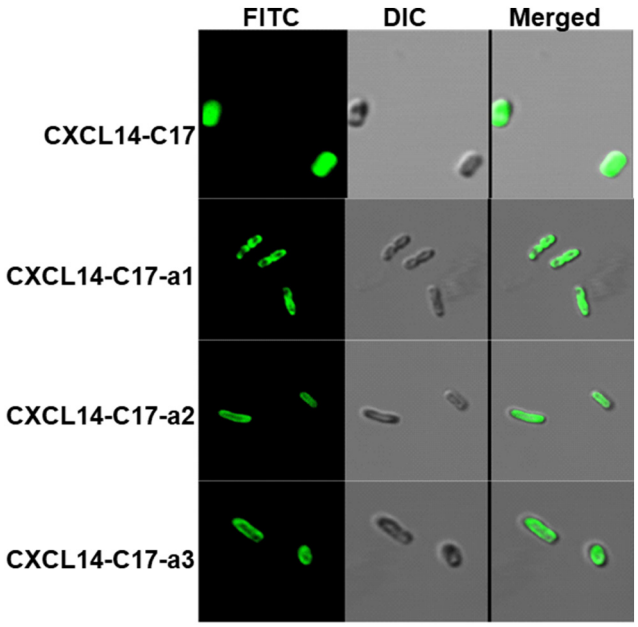

Fig. 9. Localization of fluorescein isothiocyanate (FITC) labeled 17-meric $CXCL14_{59–75}$ (CXCL14-C17) and its analogs on bacteria. Approximately 10^7 CFU of *Escherichia coli* were incubated with FITC labeled peptides (2 × MIC) for 1 h. Bacteria were washed and fixed, and images were acquired using confocal microscopy.

responses in animals. It is easily released into the host blood system from dead bacteria following antibiotic treatment of gram-negative bacterial infection [23,24]. It can induce sepsis, a leading healthcare problem affecting millions of people worldwide [25,26]. Recently, several AMPs, such as LL-37 and β-defensin, were reported to inhibit LPS-induced inflammatory response [27,28]. Prior to performing experiments involving anti-inflammatory activity, the cytotoxicity of the peptides against RAW 264.7 cells were assessed using the 3-(4,5-dimethylthiazol-2-yl)-2,5-diphenyltetrazolium bromide (MTT) assay, which is based on the reduction of MTT into formazan dye by the mitochondria of living cells. The amount of formazan produced is directly proportional to the living cells. To confirm a lack of cytotoxicity, peptides were evaluated at various concentrations (1.25 μM to 160 μM). As showed in Fig. 11, CXCL14-C17 and its analogs did not affect RAW

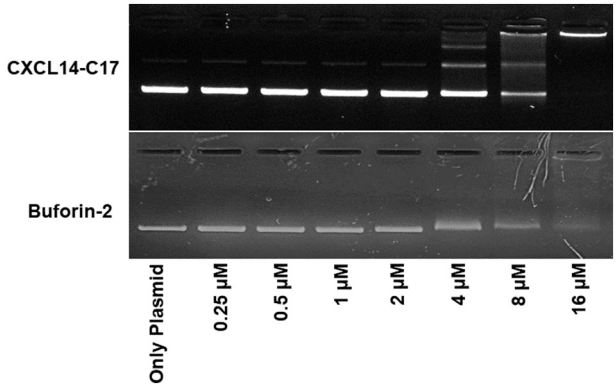

Fig. 10. Interaction of peptides with plasmid DNA from *Escherichia coli*. Binding was assayed by measuring inhibition of migration by plasmid DNA (200 ng; pBR322). DNA and peptides were co-incubated for 1 h at room temperature before electrophoresis on a 1% agarose gel.

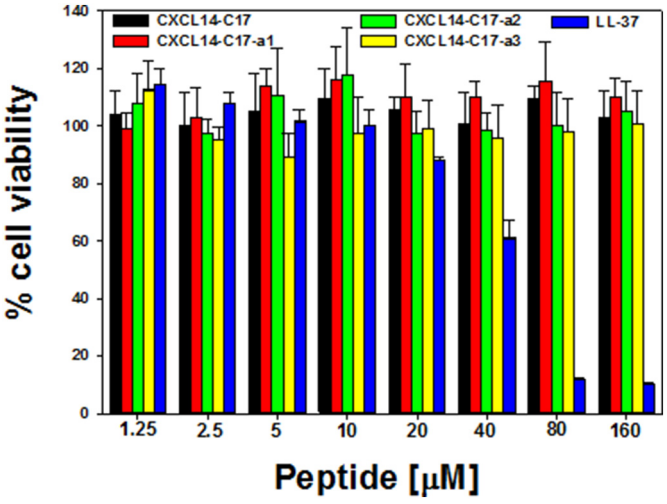

Fig. 11. Cytotoxicity of 17-meric $CXCL14_{59–75}$ (CXCL14-C17) and its analogs against mouse macrophage RAW264.7 cells. Cells were incubated with varying concentrations (1.25 to 160 μM) of CXCL14-C17 and its analogs for 48 h at 37 °C. Effects on cell viability were determined using 3-(4,5-dimethylthiazol-2-yl)-2,5-diphenyltetrazolium bromide (MTT) assay. Cell survival was calculated using the following formula: survival % = ([A550 of peptide − treated cells] / [A550 of untreated cells]) × 100.

264.7 cell viability even at a high concentration of 160 μM.

Nitric oxide (NO), tumor necrosis factor (TNF)-α, interleukin (IL)-6 and monocyte chemoattractant protein (MCP)-1 are the major inflammatory products released during bacterial infection [29]. These cytokines are produced by humans following exposure to stimuli such as LPS. To assess the effects of the peptides on LPS-stimulated proinflammatory cytokine release in RAW264.7 cells, they were treated with or without 20 ng/ml LPS in the presence of the peptides at 10 μM, 20 μM, and 40 μM. NO production can be determined in the cell supernatant using the Griess method. The release of TNF-α, IL-6, and MCP-1 was quantified using an enzyme-linked immunosorbent assay (ELISA) kit. As showed in Fig. 12, CXCL14-C17-a3 displayed high activity at 40 μM, which inhibited all the tested cytokines by nearly 100%. CXCL14-C17-a2 inhibited IL-6 and NO production by 100% at 40 μM but suppressed MCP-1 and TNF-α release by 70% and 60%, respectively. However, CXCL14-C17-a1 and CXCL14-C17 showed no or less inhibitory activity on NO, TNF-α, IL-6, and MCP-1 production at 40 μM. In addition, NO, TNF-α, IL-6, and MCP-1 were not induced by treatment with only 40 μM peptide without LPS stimulation (data not shown). Overall, the inhibition of cytokine production by the peptides was

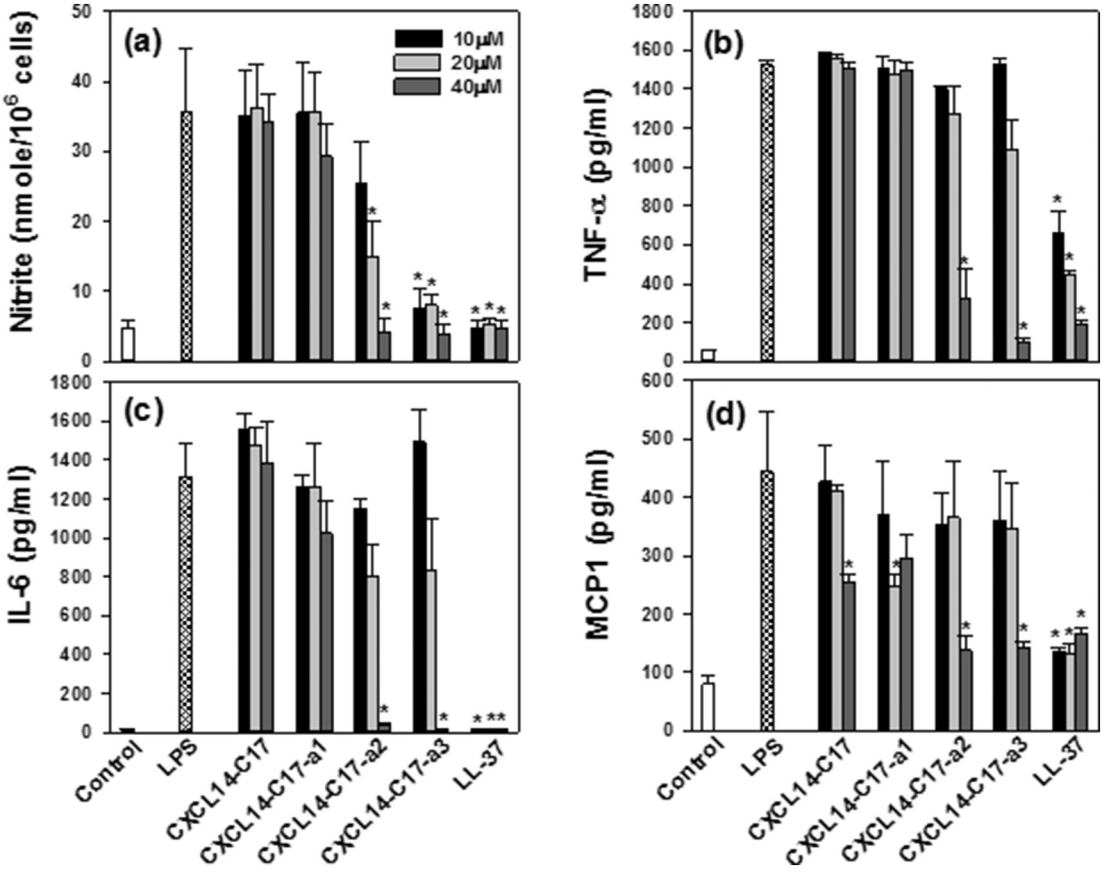

Fig. 12. Effects of peptides on release of nitric oxide (NO), tumor necrosis factor (TNF)-α, interleukin (IL)-6, and monocyte chemoattractant protein (MCP)-1 by lipopolysaccharide (LPS)-stimulated RAW264.7 cells. *Significant effects of peptides compared to LPS treated cells. Data were analyzed using one-way analysis of variance (ANOVA) with Bonferroni's post-test ($^*p < 0.001$ for each agonist). Data are means ± SEM of triplicates, and findings were similar when experiments were repeated using different cells.

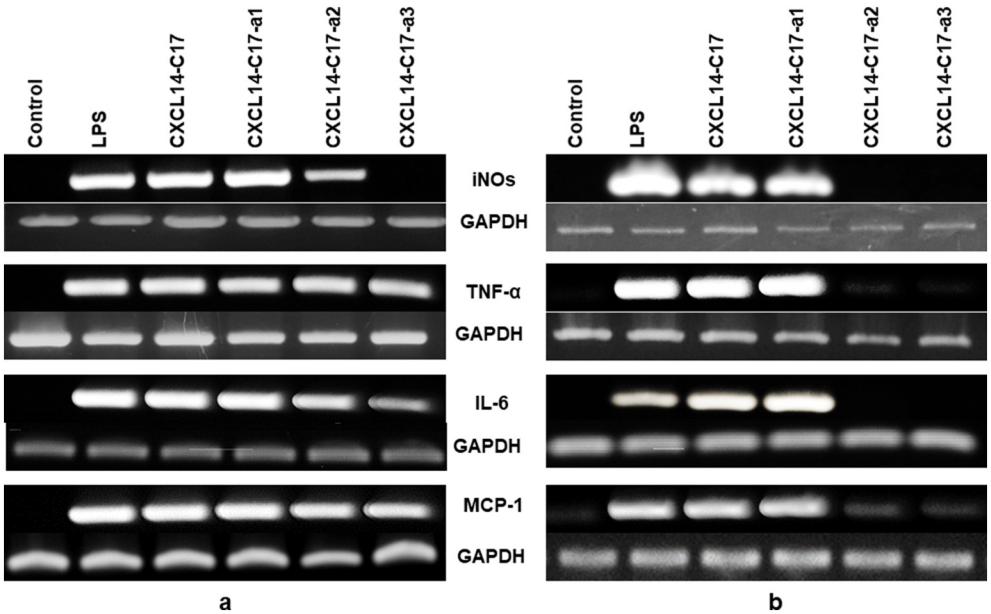

Fig. 13. Effects of 17-meric $CXCL14_{59–75}$ (CXCL14-C17) and its analogs on mRNA expression of inducible nitric oxide synthase (iNOS), tumor necrosis factor (TNF)-α, interleukin (IL)-6, and monocyte chemoattractant protein (MCP)-1 in lipopolysaccharide (LPS)-stimulated RAW264.7 cells. RAW264.7 cells (5×10^5 cells/well) were incubated with peptides at 20 (a) and 40 μM (b) concentrations in the presence of LPS (20 ng/ml) for 3 h (for TNF-α, IL-6, and MCP-1) or 6 h (for iNOS). Total RNA was isolated and analyzed to determine mRNAs levels of iNOS, TNF-α, IL-6, and MCP-1 using reverse transcription-polymerase chain reaction (RT-PCR).

ranked as follows: CXCL14-C17-a3 > CXCL14-C17-a2 > CXCL14-C17-a1 = CXCL14-C17.

To determine whether the peptides altered the production of proinflammatory cytokines, the expression of iNOS, TNF-α, IL-6, and MCP-1 mRNA was analyzed using reverse transcription-polymerase chain reaction (RT-PCR) (Fig. 13). CXCL14-C17-a2 and CXCL14-C17-a3 peptides completely inhibited the expression of iNOS, TNF-α, IL-6, and MCP-1 at 40 μM, whereas CXCL14-C17 and CXCL14-C17-a1 did not. CXCL14-C17-a3 and CXCL14-C17-a2 completely or partially inhibited the expression of iNOS at 20 μM. In contrast, CXCL14-C17 and CXCL14-

C17-a1 did not inhibit the expression of iNOS at the same concentration. Overall, the inhibition of cytokine expression by the peptides was ranked as follows: CXCL14-C17-a3 > CXCL14-C17-a2 > CXCL14-C17-a1 = CXCL14-C17. These data agree with the observed inhibition of NO, TNF-α, IL-6, and MCP-1 production by the peptides.

4. Conclusions

In summary, our results indicated that CXCL14-C17 kills bacteria by an intracellular targeting mechanism, whereas the amphipathic designed CXCL14-C17 analogs kills microbes by damaging the membrane integrity. Furthermore, we successfully designed multifunctional AMPs, CXCL14-C17-a2 and CXCL14-C17-a3, with cell selectivity, synergistic effects in combination with conventional antibiotics, salt and serum stability, anti-biofilm property, and anti-inflammatory (endotoxin-neutralizing) activity. These peptides could be developed further as novel antimicrobial and anti-inflammatory agents to treat antibiotic-resistant infections.

Conflict of interest

The authors declare that there are no conflicts of interest.

Transparency document

The http://dx.doi.org/10.1016/j.bbamem.2018.06.016 associated with this article can be found, in online version.

Acknowledgements

This work was supported by the Basic Science Research Program through the National Research Foundation of Korea (NRF) funded by the Ministry of Education (2015R1D1A1A01057988) and the National Research Foundation of Korea (NRF) grant funded by the Korea government (MSIT) (2018R1A2B6003250).

Appendix A. Supplementary data

Supplementary data to this article can be found online at https://doi.org/10.1016/j.bbamem.2018.06.016.

References

[1] L. Jing, C. Mita, S. Hannes, B. Sandra, G. Meinrad, CXCL14 as an emerging immune and inflammatory modulator, J. Inflamm. 13 (2016) 1–8.
[2] M. Wolf, B. Moser, Antimicrobial activities of chemokines: not just a side-effect? Front. Immunol. 3 (2012) 213.
[3] C. Maerki, S. Meuter, M. Liebi, K. Muhlemann, M.J. Frederick, N. Yawalkar, B. Moser, M. Wolf, Potent and broad-spectrum antimicrobial activity of CXCL14 suggests an immediate role in skin infections, J. Immunol. 182 (2009) 507–514.
[4] K. Tsuji, A. Shigenaga, Y. Sumikawa, K. Tanegashima, K. Sato, K. Aihara, T. Hara, A. Otaka, Application of N-C- or C-N-directed sequential native chemical ligation to the preparation of CXCL14 analogs and their biological evaluation, Bioorg. Med. Chem. 19 (2011) 4014–4020.
[5] G. Rajasekaran, E.Y. Kim, S.Y. Shin, LL-37-derived membrane-active FK-13 analogs possessing cell selectivity, anti-biofilm activity and synergy with chloramphenicol and anti-inflammatory activity, Biochim. Biophys. Acta Biomembr. 1859 (2017) 722–733.
[6] L.R. Mclean, K.A. Hagaman, T.J. Owen, J.L. Krstenansky, Minimal peptide length for interaction of amphipathic α-helical peptides with phosphatidylcholine liposomes, Biochemistry 30 (1991) 31–37.
[7] J.S. Khara, Y. Wang, X.Y. Ke, S. Liu, S.M. Newton, P.R. Langford, Y.Y. Yang, P.L. Ee, Antimycobacterial activities of synthetic cationic α-helical peptides and their synergism with rifampicin, Biomaterials 35 (2014) 2032–2038.
[8] R.I. Lehrer, A. Barton, K.A. Daher, S.S. Harwig, T. Ganz, M.E. Selsted, Interaction of human defensins with *Escherichia coli*. Mechanism of bactericidal activity, J. Clin. Invest. 84 (1989) 553–561.
[9] B. Skerlavaj, D. Romeo, R. Gennaro, Rapid membrane permeabilization and inhibition of vital functions of gram-negative bacteria by bactenecins, Infect. Immun. 58 (1990) 3724–3730.
[10] B.L. Roth, M. Poot, S.T. Yue, P.J. Millard, Bacterial viability and antibiotic susceptibility testing with SYTOX green nucleic acid stain, Appl. Environ. Microbiol. 63 (1997) 2421–2431.
[11] R.E. Hancock, H.G. Sahl, Antimicrobial and host-defense peptides as new anti-infective therapeutic strategies, Nat. Biotechnol. 24 (2006) 1551–1557.
[12] A. Bell, Antimalarial peptides: the long and the short of it, Curr. Pharm. Des. 17 (2011) 2719–2731.
[13] M. Katsumi, Control of cell selectivity of antimicrobial peptides, Biochim. Biophys. Acta Biomembr. 1788 (2009) 1687–1692.
[14] D. Takahashi, S.K. Shukla, O. Prakash, G. Zhang, Structural determinants of host defense peptides for antimicrobial activity and target cell selectivity, Biochimie 92 (2010) 1236–1241.
[15] G. Batoni, M. Casu, A. Giuliani, V. Luca, G. Maisetta, M.L. Mangoni, G. Manzo, M. Pintus, G. Pirri, A.C. Rinaldi, M.A. Scorciapino, I. Serra, A.S. Ulrich, P. Wadhwani, Rational modification of a dendrimeric peptide with antimicrobial activity: consequences on membrane-binding and biological properties, Amino Acids 48 (2016) 887–900.
[16] Y. Chen, C.T. Mant, M.W. Farmer, R.E. Hancock, M.L. Vasil, R.S. Hodges, Rational design of α-helical antimicrobial peptides with enhanced activities and specificity/therapeutic index, J. Biol. Chem. 280 (2005) 12316–12329.
[17] M.A. Fazio, L. Jouvensal, F. Vovelle, P. Bulet, M.T. Miranda, S. Daffre, A. Miranda, Biological and structural characterization of new linear gomesin analogues with improved therapeutic indices, Biopolymers 88 (2007) 386–400.
[18] J.T. Cheng, J.D. Hale, M. Elliot, R.E. Hancock, S.K. Straus, Effect of membrane composition on antimicrobial peptides aurein 2.2 and 2.3 from Australian southern bell frogs, Biophys. J. 96 (2009) 552–565.
[19] T. Tangden, Combination antibiotic therapy for multidrug-resistant Gram-negative bacteria, Ups. J. Med. Sci. 119 (2014) 149–153.
[20] L. Fassi Fehri, H. Wróblewski, A. Blanchard, Activities of antimicrobial peptides and synergy with enrofloxacin against *Mycoplasma pulmonis*, Antimicrob. Agents Chemother. 51 (2007) 468–474.
[21] J. Overhage, A. Campisano, M. Bains, E.C. Torfs, B.H. Rehm, R.E. Hancock, Human host defense peptide LL-37 prevents bacterial biofilm formation, Infect. Immun. 76 (2008) 4176–4182.
[22] J. Zhang, J. Huang, C. Say, R.L. Dorit, K.T. Queeney, Deconvoluting the effects of surface chemistry and nanoscale topography: *Pseudomonas aeruginosa* biofilm nucleation on Si-based substrates, J. Colloid Interface Sci. 519 (2018) 203–213.
[23] M.S. Trent, M.C. Stead, A.X. Tran, J.V. Hankins, Diversity of endotoxin and its impact on pathogenesis, J. Endotoxin Res. 12 (2006) 205–223.
[24] Y. Rosenfeld, N. Papo, Y. Shai, Endotoxin (lipopolysaccharide) neutralization by innate immunity host-defense peptides, J. Biol. Chem. 281 (2006) 1636–1643.
[25] M.E. Evans, M. Pollack, Effect of antibiotic class and concentration on the release of lipopolysaccharide from *Escherichia coli*, J. Infect. Dis. 167 (1993) 1336–1343.
[26] G.S. Martin, D.M. Mannino, S. Eaton, M. Moss, The epidemiology of sepsis in the United States from 1979 through 2000, N. Engl. J. Med. 348 (2003) 1546–1554.
[27] G. Fan, X. Jiang, X. Wu, P.A. Fordjour, L. Miao, H. Zhang, Y. Zhu, X. Gao, Anti-inflammatory activity of tanshinone IIA in LPS-stimulated RAW264.7 macrophages via miRNAs and TLR4-NF-κB pathway, Inflammation 39 (2016) 375–384.
[28] Y. Sun, D. Shang, Inhibitory effects of antimicrobial peptides on lipopolysaccharide-induced inflammation, Mediat. Inflamm. 2015 (2015) 167572.
[29] E.Y. Kim, G. Rajasekaran, S.Y. Shin, LL-37-derived short antimicrobial peptide KR-12-a5 and its d-amino acid substituted analogs with cell selectivity, anti-biofilm activity, synergistic effect with conventional antibiotics, and anti-inflammatory activity, Eur. J. Med. Chem. 136 (2017) 428–441.